

# **Stereochemical characterization of fluorinated 2-(phenanthren-1-yl)propionic acids by enantioselective high performance liquid chromatography analysis and electronic circular dichroism detection**

Carlo Bertucci \* (1), Marco Pistolozzi (1), Daniele Tedesco (1), Riccardo Zanasi (2),

Renzo Ruzziconi (3), Anna Maria Di Pietra (1)

*(1) Department of Pharmaceutical Sciences, University of Bologna, Italy;*

*(2) Department of Chemistry and Biology, University of Salerno, Italy;*

*(3) Department of Chemistry, University of Perugia, Italy.*

\* Corresponding author. Tel.: +39 051 2099 731; fax: +39 051 2099 734; email: [carlo.bertucci@unibo.it](mailto:carlo.bertucci@unibo.it)

---

*Accepted Manuscript version. The Published Journal Article is available on the Journal of Chromatography A, Volume 1232, pages 128–133 (DOI: <https://doi.org/10.1016/j.chroma.2011.10.090>). Supplementary Material available free of charge on the article webpage.*

© 2011. This Manuscript version is made available under the CC-BY-NC-ND 4.0 license.

<https://creativecommons.org/licenses/by-nc-nd/4.0/>



## Abstract

Enantioselective high performance liquid chromatography (HPLC) coupled with a detection system based on the simultaneous measurement of UV absorption and electronic circular dichroism (ECD) allows a complete stereochemical characterization of chiral compounds, once the relationship between sign of the chiroptical properties and absolute configuration is determined. In the present communication, the development of enantioselective HPLC methods for the resolution of a series of fluorinated 2-phenanthrenylpropionic acids (**1-6**) is reported. Different chiral stationary phases (CSPs) were tested: Chiralcel<sup>®</sup> OJ, Chiralcel<sup>®</sup> OD, Chiralpak<sup>®</sup> AD, (*S,S*)-Whelk-O<sup>®</sup> 1, Chirobiotic<sup>™</sup> T and  $\alpha_1$ -acid glycoprotein (AGP).

The results allow the application of the methods to a reliable determination of the enantiomeric excess for all the examined compounds; the highest enantioselectivity values were obtained with the Hibar<sup>®</sup> [(*S,S*)-Whelk-O<sup>®</sup> 1] column for some of the examined compounds. In the case of *rac*-2-(6-fluorophenanthren-1-yl)propionic acid (**1**), the relationship between circular dichroism and absolute configuration of the enantiomeric fractions was determined by ECD analysis and time-dependent density functional theory (TD-DFT) calculations.

The experimental ECD spectrum of the second-eluted fraction of **1** on the Hibar<sup>®</sup> [(*S,S*)-Whelk-O<sup>®</sup> 1] column was found to be in excellent agreement with the theoretical ECD spectrum of (*S*)-**1**; therefore, the absolute configuration of the first- and second-eluted enantiomers on the (*S,S*)-Whelk-O<sup>®</sup> 1 CSP was assessed as (*R*) and (*S*), respectively, and the elution orders of the enantiomeric forms of **1** were determined on all the different CSPs.

## 1. Introduction

Fluorinated profens have received particular consideration in reference to their biological activity as successful non-steroidal anti-inflammatory drugs (NSAIDs), especially in connection with the

presence of fluorine in the molecule. In fact, once placed in a specific position of a bioactive molecule, fluorine can substantially affect its chemical stability [1-6], thus slackening the related metabolic processes. Moreover, since the C-F bond is stronger than the C-H bond and exhibits reverse polarity, replacement of the  $\alpha$ -hydrogen with the quasi-isosteric fluorine conveys a higher configurational stability to the chiral center of profens [7], thus allowing the drug pharmacodynamics, as well as the stereochemical matching with the biological target, to be investigated.

Since the biological activity of 2-(phenanthren-1-yl)propionic acid as a NSAID was reported to be similar to that of fenbufen [8], a number of nucleus and/or side-chain fluorinated 2-phenantrylpropionic acids were prepared [9], in order to assess the effect of fluorine on the structure/activity relationship with respect to its position and to the configuration of the chiral carbon. Nevertheless, a reliable study on the relationship between stereochemistry and biological activity requires a full stereochemical characterization of the compounds under investigation.

In this article, the development of enantioselective high performance liquid chromatography (HPLC) methods for the resolution of a series of 2-(fluorophenanthren-1-yl)propionic acids (**1-6**, Figure 1) is reported; these methods may be applied for the determination of the enantiomeric excess (e.e.).

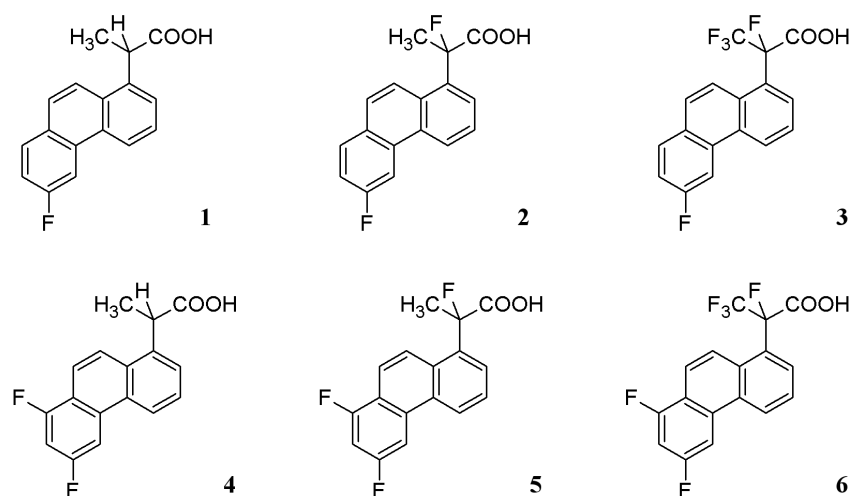


**Figure 1.** 2-(fluorophenanthren-1-yl)propionic acids.

For one of these compounds, 2-(6-fluorophenanthren-1-yl)-propionic acid (**1**), the enantioselective method has been scaled up to allow the collection of the enantiomeric fractions, before their stereochemical characterization. The e.e. value was determined through the same chromatographic assay, and the absolute configuration was assessed by electronic circular dichroism (ECD) spectroscopy and time-dependent density functional theory (TD-DFT) computations.

## 2. Experimental

### 2.1. Materials

Compounds **1-6** were prepared as previously reported [9]. n-Hexane, acetonitrile, methanol, ethanol, 1-propanol, 2-propanol, glacial acetic acid, formic acid, triethanolamine and triethylamine were purchased from Sigma-Aldrich (Milan, Italy). All solvents used to prepare solutions and mobile phases were HPLC or analytical grade.  $K_2HPO_4$  and  $KH_2PO_4$  powders were purchased from Carlo Erba Reagenti (Milan, Italy). Water was doubly distilled and buffers were filtered through a 0.22  $\mu$ m membrane filter.

### 2.2. HPLC analysis

#### *2.2.1. Instrumentation*

A Varian (Palo Alto, CA, USA) Mod. 5000 HPLC system with a HP 1040A diode array detector (Hewlett Packard, Waldbronn, Germany) was used for the development of enantioselective methods and the collection of enantiomeric fractions. The e.e. determination with simultaneous monitoring of UV and ECD signals of compound **1** were carried out using a Jasco (Tokyo, Japan) HPLC system consisting of a Jasco PU-980 pump, a Jasco MD 910 multiwavelength detector and a CD-995 chiral detector, equipped with a 25 mm pathlength HPLC flow cell. Samples were injected by a 20  $\mu$ L loop in both instruments.

The following HPLC columns were used, having different chiral stationary phases (CSPs): Chiralcel® OJ (250 × 4.6 mm I.D., 10 µm) and Chiralpak® AD (250 × 4.6 mm I.D., 10 µm), purchased from Daicel, Chiral Technologies Europe, Illkirch, France; Chiralcel® OD (250 × 4.6 mm I.D., 10 µm; Daicel, Millinckrodt Baker B.V., Deventer, Holland); Hibar® pre-packed column RT (250 × 4.6 mm I.D., 5 µm, customized packing (S,S)-Whelk-O® 1; Merck KGaA, Darmstadt, Germany); Chirobiotic™ T (250 × 4.6 mm I.D., 5 µm; Astec, Whippany, NJ, USA), and Chiral-AGP (100 × 4.0 mm I.D., 5 µm; ChromTech AB, Sollentuna, Sweden).

### 2.2.2. Chromatographic conditions

Stock solutions of compounds **1-6** (1.0 mg mL<sup>-1</sup>) in 2-propanol and in methanol were prepared for direct-phase and reversed-phase chromatography, respectively. Stock solutions were further diluted in the same solvents to a concentration range between 0.02 and 0.1 mg mL<sup>-1</sup>.

Mobile phases used in direct-phase chromatography were prepared with hexane and 2-propanol, adding formic acid or acetic acid to improve the chromatographic resolution. In particular, hexane/2-propanol/acetic acid mobile phases were used with Chiralcel® OJ (79:20:1; 79.5:20:0.5; 69:30:1; 89.5:10:0.5; 80:20:0, v/v/v), and Hibar® [(S,S)-Whelk-O® 1] columns (80:20:0; 79.5:20:0.5; 90:10:0; 89.5:10:0.5; 94.5:5:0.5, v/v/v), while hexane/2-propanol/formic acid mobile phases were used with Chiralcel® OD (69.5:30:0.5; 79.5:20:0.5; 89.5:10:0.5, v/v/v) and Chiralpak® AD (70:30:0; 69.5:30:0.5, v/v/v) columns.

The Chiralcel® OD column was also successfully used to separate and collect the single enantiomers of compound **1** (mobile phase, 79.5:20:0.5, v/v/v hexane/2-propanol/formic acid; flow 1 mL min<sup>-1</sup>, λ: 250 nm). The e.e. of each fraction of **1** was determined by using the (S,S)-Whelk-O® 1 CSP (mobile phase, 79.5:20:0.5 v/v/v hexane/2-propanol/acetic acid; flow 1 mL min<sup>-1</sup>, λ: 295 nm). The enantiomeric fractions were dried under nitrogen, reconstituted with 2-propanol and analyzed by UV spectroscopy to determine their concentration.

In reversed-phase chromatography, solutions of triethylamine (TEA) acetate buffer at different pH values mixed with methanol or acetonitrile and phosphate buffer/1-propanol (PB) were used with Chirobiotic™ and Chiral-AGP columns, respectively.

Triethylamine (TEA) acetate buffer was prepared adding acetic acid to aqueous triethylamine to adjust the pH value. The following mobile phases were used: TEA acetate (20 mM, pH 5, 6 and 7)/methanol 90:10, v/v; TEA acetate (20 mM, pH 6)/methanol (75:25; 80:20; 95:5, v/v); TEA acetate (20 mM, pH 6)/acetonitrile (80:20; 90:10; 95:5, v/v). Replacement of triethylamine by triethanolamine did not show any significant difference. Phosphate buffer (PB, 0.1 M, pH 6) was obtained by adding a 0.1 M aq.  $\text{KH}_2\text{PO}_4$  (pH ~ 4) to 0.1 M aq.  $\text{K}_2\text{HPO}_4$  (pH ~ 9). Mobile phases consisted in PB/1-propanol mixtures (90:10; 95:5, v/v). All mobile phases were degassed by sonication. Flow rate was maintained between 0.6 and 1.5 mL min<sup>-1</sup>.

The enantioselectivity ( $\alpha$ ) was calculated as  $\alpha = k'_2 / k'_1$ , where  $k'_2$  and  $k'_1$  are the capacity factors of the second- and first-eluted enantiomers, respectively. Capacity factors ( $k'$ ) are defined as  $k' = \frac{t_r - t_0}{t_0}$ , where  $t_r$  is the retention time of the analyte, and  $t_0$  is the retention time of a non-

retained solute. The enantiomeric excess was determined as  $\text{e.e.} = \frac{[A] - [B]}{[A] + [B]} \cdot 100$ , where [A] and [B] are the peak areas of the most and less abundant enantiomers, respectively.

### 2.3. UV and ECD measurements

UV spectra of compounds **1-6** were carried out on a spectrophotometer Jasco V-520, in 2-propanol at room temperature, using 1 cm pathlength cells. ECD spectra (370 – 210 nm spectral range) of the single enantiomeric fractions of **1** were recorded on a Jasco J-810 spectropolarimeter, in 2-propanol at room temperature, using a 1 cm pathlength cell. Concentrations were adjusted to keep the absorbance in the optimum photometric range. Spectra were recorded at 0.5 nm intervals

using a 2 nm spectral bandwidth, a 20 nm min<sup>-1</sup> scan rate and a 4 sec time constant. The actual concentration of the fractions of **1** were determined by UV analysis.

#### 2.4. Conformational analysis and ECD calculation

Molecular mechanical (MM) calculations were carried out for a preliminary conformational analysis of (*S*)-**1** (Figure 2). The conformer distribution was determined at the MMFF94s [10] level using the Spartan'02 software, [11] and the relative energies ( $\Delta E_{\text{MM}}$ ) with respect to the lowest-energy conformation were calculated for each conformer.

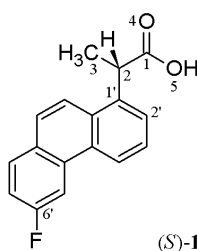


**Figure 2.** (2*S*)-2-(6-fluorophenanthren-1-yl)propionic acid [(*S*)-**1**].

Full quantum mechanical (QM) geometry optimizations were then performed through density functional theory (DFT) [12,13] calculations on the MM conformers having  $\Delta E_{\text{MM}} \leq 3$  kcal mol<sup>-1</sup>, using the Gaussian 09 software package. [14] The hybrid B3LYP exchange-correlation functional [15-18] was used in combination with the triple-zeta, double-polarization TZ2P basis set; [19-20] solvent effects were accounted for 2-propanol by adopting the polarizable continuum model (PCM) in its integral equation formalism, [21] as implemented within the Gaussian 09 package. The Boltzmann distribution of conformers at 298.15 K and 1 atm was calculated from relative self-consistent field energies ( $\Delta E_{\text{QM}}$ ), and relative free energies ( $\Delta G$ ).

Time-dependent DFT (TD-DFT) [22] calculations of the chiroptical properties of (*S*)-**1** were performed at the B3LYP/TZ2P level on the optimized geometries of conformers with  $\Delta E_{\text{QM}} \leq 3$  kcal mol<sup>-1</sup>; excitation wave numbers ( $\sigma_{mn}$ ) and rotational strengths ( $R_{mn}$ ) were determined for the lowest 50 excited states of each conformer. Theoretical ECD spectra as a function of wave number [ $\Delta \epsilon(\sigma)$ ] were derived for (*S*)-**1** by approximation of all  $R_{mn}$  values to

Gaussian functions ( $\Delta\sigma = 0.3\text{ eV}$ ), summation over all excited states and conformational averaging, according to the Boltzmann distribution of conformers. [23,24]

Theoretical spectra were converted in wavelength scale for a convenient comparison with experimental data; the correlation between the theoretical ECD spectrum of (*S*)-**1** and the experimental ECD spectra of the enantiomeric fractions of **1** was then evaluated by the Pearson product-moment correlation coefficient ( $r$ ). [25]

### 3. Results and discussion

#### *3.1. Enantioselective HPLC analysis*

The development of enantioselective assays to determine the e.e. values for the series of 2-(fluorophenanthren-1-yl)propionic acids required the screening of several CSPs and various experimental conditions. Among the various direct-mode columns tested, Chiralcel® OJ proved to be efficient in the resolution of compounds **1**, **2** and **4** (Tables 1, S.1).

**Table 1.** Resume of the best chromatographic conditions and parameters for the separation of racemic mixtures of compounds **1-6**.

| Column                               | Compound | Mobile phase                                     | $t_0$ (min) | $k'_1$ | $\alpha$ |
|--------------------------------------|----------|--|-------------|--------|----------|
| Chiralcel®OJ                         | <b>1</b> | hexane/2-propanol/acetic acid 69:30:1, v/v/v     | 2.89        | 1.51   | 1.16     |
|                                      | <b>2</b> |  |             | 1.97   | 1.74     |
| Chiralcel®OJ                         | <b>4</b> | hexane/2-propanol/acetic acid 79.5:20:0.5, v/v/v | 2.89        | 1.08   | 1.32     |
| Chiralcel®OD                         | <b>1</b> | hexane/2-propanol/formic acid 69:30:1, v/v/v     | 3.23        | 0.60   | 1.30     |
| Chiralpak®AD                         | <b>2</b> | hexane/2-propanol/formic acid 69:30:1, v/v/v     | 3.49        | 1.37   | 1.23     |
| Hibar®<br>[( <i>S,S</i> )Whelk-O® 1] | <b>1</b> | hexane/2-propanol/acetic acid 79.5:20:0.5, v/v/v | 2.80        | 1.45   | 2.15     |
|                                      | <b>2</b> |  |             | 0.84   | 2.05     |
|                                      | <b>4</b> |  |             | 0.93   | 2.07     |
|                                      | <b>5</b> |  |             | 0.59   | 1.83     |
| Chiral-AGP                           | <b>1</b> | PB (0.1 M, pH 6)/1-propanol 95:5, v/v            | 2.08        | 7.51   | 1.56     |
|                                      | <b>2</b> |  |             | 5.69   | 1.79     |
|                                      | <b>3</b> |  |             | 10.95  | 1.53     |
|                                      | <b>4</b> |  |             | 8.54   | 1.19     |
|                                      | <b>5</b> |  |             | 4.71   | 2.70     |
|                                      | <b>6</b> |  |             | 14.51  | 2.44     |
| Chirobiotic™ T                       | <b>1</b> | TEA acetate (20 mM, pH 6)/methanol 75:25, v/v    | 3.33        | 1.63   | 1.15     |



The mobile phases were prepared with hexane and 2-propanol, adding acetic acid to improve the efficiency of the separation process. The increase in 2-propanol concentration determined a significant decrease in retention times, while the enantioselectivity did not change significantly (Table S.1). Chiralcel® OD was successfully employed in the enantiomeric resolution of compounds **1** while Chiralpak® AD was effective in resolving compound **2** (Tables 1, S.2, S.3). Changes in both the nature of the mobile phase and the flow rate, did not allow the resolution of the other compounds of the series (Tables S.2, S.3). The Hibar® [(*S,S*)-Whelk-O® 1] column was efficient for the enantiomeric resolution of most of the 2-(fluorophenanthren-1-yl)propionic acids under investigation (Tables 1, S.4). As an example, the enantiomeric resolution of *rac*-**4** is shown in Figure 3. Higher polarity of the mobile phase caused a significant reduction in retention times (Table S.4). This CSP resulted particularly efficient and suitable to determine the e.e. values of enriched fractions of these compounds.

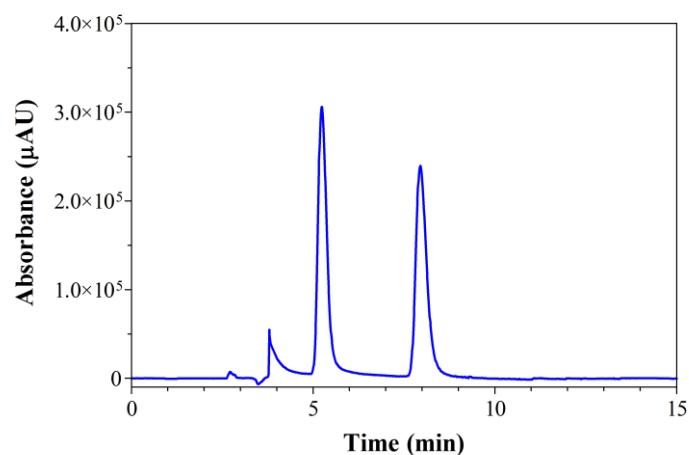


**Figure 3.** Chromatogram relative to the enantioresolution of *rac*-**4**, 0.1 mg mL<sup>-1</sup>, obtained on Hibar® [(*S,S*)-Whelk-O® 1] column. Mobile phase: *n*-hexane/2-propanol/acetic acid 79.5:20:0.5, v/v/v, flow 1 mL min<sup>-1</sup>; UV detection ( $\lambda$  = 250 nm).

AGP proved to be a very efficient reversed-phase CSP in resolving all the examined compounds (Tables 1, S.5), while Chirobiotic™ T was effective in the resolution of compound **1** (Tables 1, S.6). In the case of AGP, the interaction of the analytes with the chiral selector was strongly affected by the concentration of the organic modifier in the mobile phase, as shown by the

significant reduction in  $k'$  and  $\alpha$  values as the 2-propanol content increases from 5 to 10% (Table S.5).

The elution of *rac*-**1** on the Hibar<sup>®</sup> [(*S,S*)-Whelk-O<sup>®</sup> 1] column was monitored by the simultaneous measurements of both absorption and ECD signals (Figure 4). [26] The chromatographic profiles obtained by monitoring the ECD signal showed a different sign of the two peaks, as a result of the enantiomeric ECD signals of the single enantiomers. The analysis performed on both Hibar<sup>®</sup> [(*S,S*)-Whelk-O<sup>®</sup> 1] and Chiral-AGP columns exhibited a reverse elution order of the enantiomers of **1** with respect to Chiralcel<sup>®</sup> OJ and Chiralcel<sup>®</sup> OD.

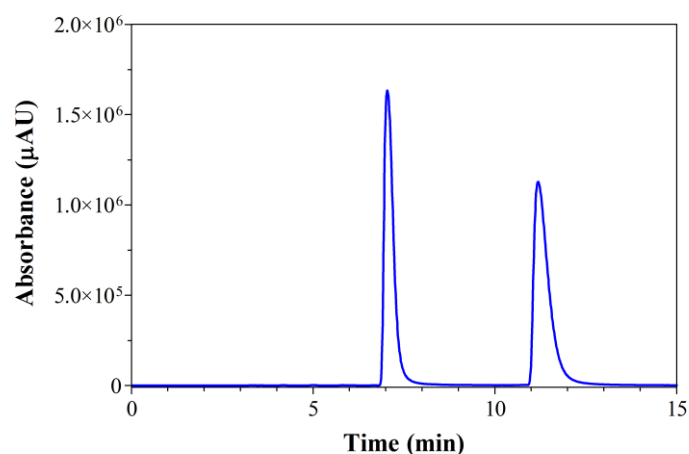


**Figure 4.** Chromatogram relative to the enantioresolution of *rac*-**1**, 1 mg mL<sup>-1</sup>, obtained on Hibar<sup>®</sup> [(*S,S*)-Whelk-O<sup>®</sup> 1] column. Mobile phase: *n*-hexane/2-propanol/acetic acid 79.5:20:0.5, v/v/v, flow 1 mL min<sup>-1</sup>; UV detection ( $\lambda$  = 250 nm).

### 3.2 Absolute configuration assignment to the enantiomers of **1**

The enantiomeric fractions of **1** were obtained by preparative enantioselective HPLC on a Chiralcel<sup>®</sup> OD column. Repetitive injections and collection of the enantiomeric fractions yielded about 0.3 mg of each enantiomer. The e.e. resulted 97.3 and 97.4% for the first- and second-eluted fraction, respectively, as determined by the chromatographic assay developed on the Hibar<sup>®</sup> [(*S,S*)-Whelk-O<sup>®</sup> 1] column (Figure 5).

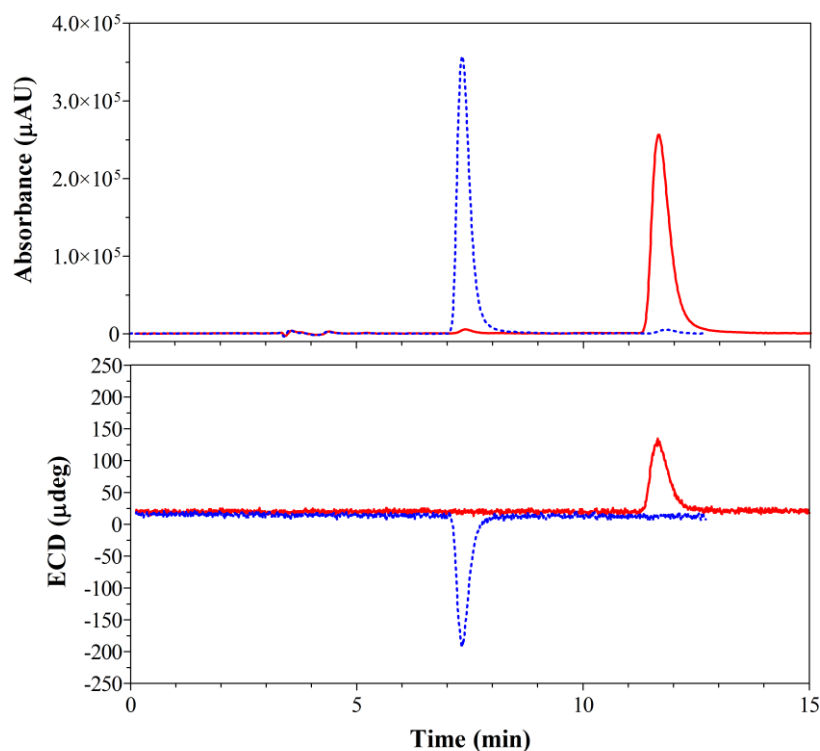


**Figure 5.** Enantiomeric excess determination for the enantiomeric fractions of **1**. *Dashed*, first-eluted fraction. *Solid*, second-eluted fraction. 1 mg mL<sup>-1</sup>, obtained on Hibar® [(*S,S*)-Whelk-O® 1] column. Mobile phase: *n*-hexane/2-propanol/acetic acid 79.5:20:0.5, v/v/v, flow 1 mL min<sup>-1</sup>; simultaneous UV and ECD detection ( $\lambda = 295$  nm).

The experimental ECD spectra were carried out by analyzing the reconstituted solutions in 2-propanol. The UV absorption spectra, as well as the specular ECD spectra, (Figure 6) show three structured bands, the lowest-energy one in the 350–320 nm spectral region, the second one in the 280–250 nm region, and the highest energy one centered at about 230 nm. The absolute configuration of the enantiomers of **1** was then determined by comparison of the experimental ECD spectra of the two fractions with the theoretical ECD spectrum calculated for (*S*)-**1**. [23] The latter was obtained by conformational averaging, taking into account the contributions of the lowest-energy conformations and their populations.

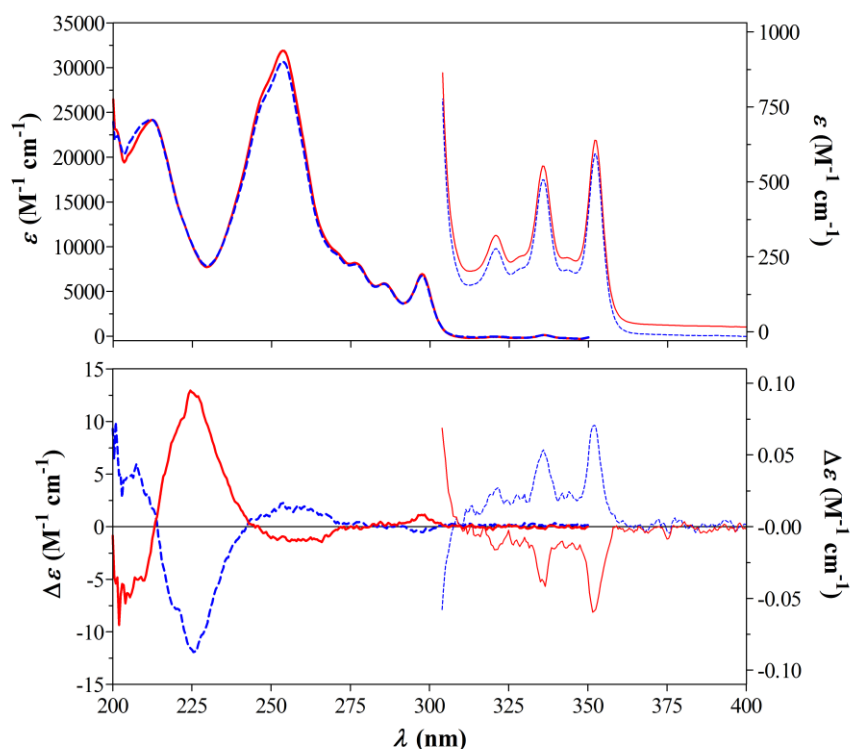


**Figure 6.** UV and ECD spectra for the enantiomeric fractions of **1** in 2-propanol (pathlength: 1 cm). *Dashed*, first-eluted fraction (400 – 300 nm: 711  $\mu\text{M}$ ; 350 – 200 nm: 17.8  $\mu\text{M}$ ). *Solid*, second-eluted fraction (400 – 300 nm: 646  $\mu\text{M}$ ; 350 – 200 nm: 16.2  $\mu\text{M}$ ). Elution order determined on Hibar® [(*S,S*)-Whelk-O® 1] column.

The conformational flexibility of the propionic moiety may be conveniently described by two dihedral angles:  $\phi_1$  (C1-C2-C1'-C2'), describing the rotation about the C2-C1' bond and to the mutual orientation of the propionic and fluorophenanthrenyl moieties and  $\phi_2$  (O4-C1-C2-C1'), describing the rotation about the C1-C2 bond and the orientation of the carboxyl group. The conformational analysis at the MM level led to the identification of seven conformers (**a-g**, Table 2) with  $\Delta E_{\text{MM}} \leq 3 \text{ kcal mol}^{-1}$ . DFT geometry optimization caused some MM conformers to converge to the same geometry: conformational clustering was carried out with a threshold RMSD value of 0.01 Å (Tables S.7, S.8). As a result, four conformers (**h-k**, Table 3) were obtained by calculations without solvation models (gas phase), while six conformers (**l-q**, Table 4) were obtained by calculations with IEFPCM for 2-propanol. Graphical representations of the different conformers are reported in the supporting information (Figures S.1, S.2).

**Table 2.** Geometrical parameters, energy values and fractional equilibrium populations for the conformers of (S)-**1**, as obtained after MM conformational analysis.

| Conformer | $\phi_1$<br>(deg) | $\phi_2$<br>(deg) | $E_{MM}$<br>(kcal mol <sup>-1</sup> ) | $\Delta E_{MM}$<br>(kcal mol <sup>-1</sup> ) | $\chi^{MM^a}$ |
|-----------|-------------------|-------------------|---------------------------------------|--|---------------|
| <b>1a</b> | -96.543           | 57.372            | 49.432                                | 0.000  | 0.3064        |
| <b>1b</b> | 123.030           | 121.692           | 49.503                                | 0.071  | 0.2718        |
| <b>1c</b> | -45.365           | 99.875            | 49.824                                | 0.392  | 0.1581        |
| <b>1d</b> | -101.334          | -114.372          | 49.868                                | 0.436  | 0.1468        |
| <b>1e</b> | 121.244           | -40.141           | 50.395                                | 0.963  | 0.0603        |
| <b>1f</b> | -46.781           | -11.567           | 50.455                                | 1.023  | 0.0545        |
| <b>1g</b> | 125.385           | 141.077           | 52.379                                | 2.947  | 0.0021        |

<sup>a</sup> Calculated using Boltzmann statistics at 298.15 K.

**Table 3.** Geometrical parameters, energy values and fractional equilibrium populations for the conformers of (S)-**1**, as obtained after DFT geometry optimization (B3LYP/TZ2P) in gas phase.

| Conformer | $\phi_1$<br>(deg) | $\phi_2$<br>(deg) | $E_{QM}$<br>(Ha/particle) | $\Delta E_{QM}$<br>(kcal mol <sup>-1</sup> ) | $\chi^{QM^a}$ | $G$<br>(Ha/particle) | $\Delta G$<br>(kcal mol <sup>-1</sup> ) | $\chi^G^a$ |
|-----------|-------------------|-------------------|---------------------------|--|---------------|----------------------|---|------------|
| <b>1h</b> | -41.419           | -81.720           | -906.29110978             | 0.000  | 0.5304        | -906.078785          | 0.000                                   | 0.7250     |
| <b>1i</b> | 122.935           | 130.731           | -906.29042587             | 0.429  | 0.2570        | -906.077137          | 1.034                                   | 0.1265     |
| <b>1j</b> | -104.315          | -119.335          | -906.29017972             | 0.584  | 0.1981        | -906.077240          | 0.970                                   | 0.1411     |
| <b>1k</b> | 120.133           | -43.138           | -906.28771135             | 2.133  | 0.0145        | -906.074447          | 2.722                                   | 0.0073     |

<sup>a</sup> Calculated using Boltzmann statistics at 298.15 K.

**Table 4.** Geometrical parameters, energy values and fractional equilibrium populations for the conformers of (S)-**1**, as obtained after DFT geometry optimization (B3LYP/TZ2P) in 2-propanol (IEFPCM solvation model).

| Conformer | $\phi_1$<br>(deg) | $\phi_2$<br>(deg) | $E_{QM}$<br>(Ha/particle) | $\Delta E_{QM}$<br>(kcal mol <sup>-1</sup> ) | $\chi^{QM^a}$ | $G$<br>(Ha/particle) | $\Delta G$<br>(kcal mol <sup>-1</sup> ) | $\chi^G^a$ |
|-----------|-------------------|-------------------|---------------------------|--|---------------|----------------------|---|------------|
| <b>1l</b> | -41.796           | 106.466           | -906.30098721             | 0.000  | 0.4037        | -906.088983          | 0.000                                   | 0.6203     |
| <b>1m</b> | 122.927           | 135.824           | -906.30034049             | 0.406  | 0.2035        | -906.087263          | 1.079                                   | 0.1003     |
| <b>1n</b> | -104.913          | 37.596            | -906.30030519             | 0.428  | 0.1960        | -906.087626          | 0.852                                   | 0.1474     |
| <b>1o</b> | -105.572          | -127.412          | -906.29999385             | 0.623  | 0.1409        | -906.087346          | 1.027                                   | 0.1095     |
| <b>1p</b> | 120.389           | -37.949           | -906.29879378             | 1.376  | 0.0395        | -906.085608          | 2.118                                   | 0.0174     |
| <b>1q</b> | 121.161           | 142.346           | -906.29795970             | 1.900  | 0.0163        | -906.084450          | 2.844                                   | 0.0051     |

<sup>a</sup> Calculated using Boltzmann statistics at 298.15 K.

The optimized conformers showed different theoretical ECD profiles (Figures S.3, S.4; rotational strengths and excitation energies in the 340 – 200 nm range are reported in Tables S.9 and S.10); this behavior is consistent with the different orientations of the phenanthrenyl chromophore with respect to the propionic moiety. Conformationally-averaged ECD spectra differ when Boltzmann populations are calculated from  $\Delta E_{\text{QM}}$  or  $\Delta G$ ; a stronger contribution of the lowest-energy conformer is observed for  $\Delta G$ -based calculations, leading to increased intensities of the short-wavelength ECD bands. Implementation of IEFPCM for long-range solvent effects in TD-DFT calculations caused minimal changes in the conformationally-averaged ECD spectrum of (*S*)-**1** (Figure S.5), mainly consisting in a slight shift towards shorter wavelengths.

The comparison between the theoretical ECD spectrum of (*S*)-**1** and the experimental spectra of the enantiomeric fractions of **1** (Figure 7) on the (*S,S*)-Whelk-O<sup>®</sup> 1 CSP shows a positive correlation between theoretical and experimental data for the second-eluted fraction, and a negative correlation for the first-eluted fraction (Table S.11). Better *r* values are obtained when  $\Delta E_{\text{QM}}$ -based Boltzmann populations are used for the conformational averaging of the theoretical ECD spectrum. Further improvement in correlation coefficients would be obtained by shifting the theoretical ECD spectrum of (*S*)-**1** towards shorter wavelengths, which is consistent with the tendency of TD-DFT calculations to underestimate transition energies. [23] On this basis, the first- and second-eluted fractions on the (*S,S*)-Whelk-O<sup>®</sup> 1 CSP are identified as the (*R*)- and (*S*)-enantiomers of **1**, respectively.

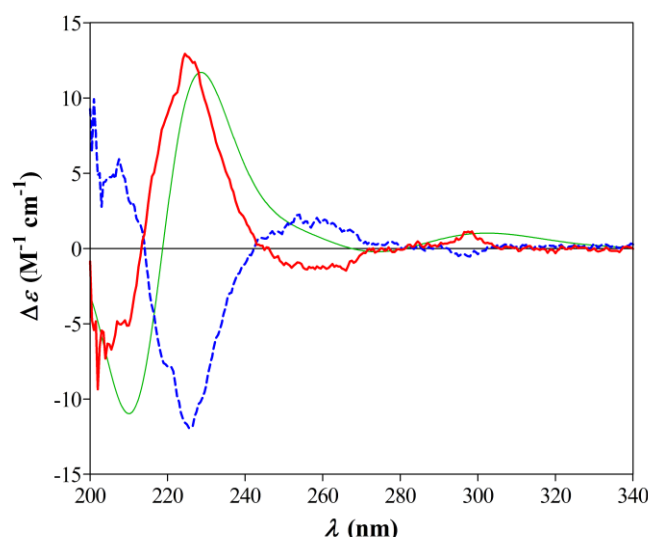


**Figure 7.** Theoretical ECD spectrum for (*S*)-**1** and comparison with experimental data. *Thin*, theoretical ECD spectrum in 2-propanol (IEFPCM solvation model,  $\Delta E_{\text{QM}}$ -based conformational averaging,  $\Delta\sigma = 0.3 \text{ eV}$ ). *Dashed*, first-eluted enantiomeric fraction of **1**. *Solid*, second-eluted enantiomeric fraction of **1**. Elution order determined on Hibar<sup>®</sup> [(*S,S*)-Whelk-O<sup>®</sup> 1] column.

Once the relationship between ECD and absolute configuration was established, it was possible to determine the elution orders for compound **1** not only on the (*S,S*)-Whelk-O<sup>®</sup> 1 CSP, but also on the other CSPs employed in the present investigation. In particular, the absolute configuration (*S*) can be assigned to the first-eluted enantiomer of **1** on Chiralcel<sup>®</sup> OJ and Chiralcel<sup>®</sup> OD, and to the second-eluted enantiomer on Chiral-AGP.

## 4. Conclusions

The developed enantioselective HPLC methods resulted efficient for the resolution of all the racemic mixtures under examination. Relatively high values of enantioselectivity were obtained on the Hibar<sup>®</sup> [(*S,S*)-Whelk-O<sup>®</sup> 1] and Chiral-AGP columns. The method was successfully scaled-up on the Chiralcel<sup>®</sup> OD column, allowing to collect the enantiomeric fractions of **1** with high values of enantiomeric excess. Full stereochemical characterization of **1** was carried out by a combination of experimental ECD spectroscopy and theoretical TD-DFT calculations, which allowed to assign (*R*) and (*S*) absolute configuration to the first- and second-eluted enantiomers of **1** on the

(*S,S*)-Whelk-O<sup>®</sup> 1 CSP, respectively. The elution order on the different CSPs were determined according to the detected ECD sign at 295 nm, which is negative for the (*R*)-enantiomer and positive for the (*S*)-enantiomer. This multi-technique approach proves to be very promising and may be applied for the stereochemical characterization of several compounds of biological and pharmaceutical interest.

## Acknowledgements

The authors are grateful for financial support from the Universities of Bologna, Salerno and Perugia and from MIUR, Italy (PRIN 2008 National Program).

## References

- [1] M. Schlosser, in: V.A. Soloshonok (Ed.), *Enantiocontrolled Synthesis of Fluoro-Organic Compounds: Stereochemical Challenges and Biomedical Targets*, Wiley, Chichester, 1999.
- [2] M. Schlosser, *Angew. Chem. Int. Ed.* 37 (1998) 1496-1513.
- [3] M. Schlosser, D. Michel, *Tetrahedron* 52 (1996) 99-108.
- [4] M. Schlosser, *Tetrahedron* 34 (1978) 3-17.
- [5] T. Welch, S. Eswarakrishnan, *Fluorine in Bioorganic Chemistry*, Wiley, New York, 1991.
- [6] R. Filler, Y. Kobayashi (Eds.), *Biomedical Aspects of Fluorine Chemistry*, Kodansha, Tokyo/Elsevier Biomedical, Amsterdam, 1982.
- [7] S.J. Hamman, *Fluorine Chem.* 60 (1993) 225-232.
- [8] A. Eirín, F. Fernández, G. Gómez, C. López, A. Santos, J.M. Calleja, D. de la Iglesia, E. Cano, *Arch. Pharm. (Weinheim)* 320 (1987) 1110-1118.



- [9] G. Ricci, R. Ruzziconi, *J. Org. Chem.* 70 (2005) 611-623.
- [10] T.A. Halgren, *J. Comput. Chem.* 20 (1999) 720-729.
- [11] Spartan'02, Wavefunction, Inc., Irvine CA, USA.
- [12] P. Hohenberg, W. Kohn, *Phys. Rev.* 136 (1964) B864-B871.
- [13] W. Kohn, L.J. Sham, *Phys. Rev.* 140 (1965) A1133-A1138.
- [14] Gaussian 09, Revision A.02, M.J. Frisch, G.W. Trucks, H.B. Schlegel, G.E. Scuseria, M.A. Robb, J.R. Cheeseman, G. Scalmani, V. Barone, B. Mennucci, G.A. Petersson, H. Nakatsuji, M. Caricato, X. Li, H.P. Hratchian, A.F. Izmaylov, J. Bloino, G. Zheng, J.L. Sonnenberg, M. Hada, M. Ehara, K. Toyota, R. Fukuda, J. Hasegawa, M. Ishida, T. Nakajima, Y. Honda, O. Kitao, H. Nakai, T. Vreven, J.A. Montgomery, Jr., J.E. Peralta, F. Ogliaro, M. Bearpark, J.J. Heyd, E. Brothers, K.N. Kudin, V.N. Staroverov, R. Kobayashi, J. Normand, K. Raghavachari, A. Rendell, J.C. Burant, S.S. Iyengar, J. Tomasi, M. Cossi, N. Rega, J.M. Millam, M. Klene, J.E. Knox, J.B. Cross, V. Bakken, C. Adamo, J. Jaramillo, R. Gomperts, R.E. Stratmann, O. Yazyev, A.J. Austin, R. Cammi, C. Pomelli, J.W. Ochterski, R.L. Martin, K. Morokuma, V.G. Zakrzewski, G.A. Voth, P. Salvador, J.J. Dannenberg, S. Dapprich, A.D. Daniels, O. Farkas, J.B. Foresman, J.V. Ortiz, J. Cioslowski, D.J. Fox, Gaussian, Inc., Wallingford CT, 2009.
- [15] A.D. Becke, *J. Chem. Phys.* 98 (1993) 5648-5652;
- [16] C. Lee, W. Yang, R.G. Parr, *Phys. Rev.* 37 (1988) B785-B789.
- [17] S.H. Vosko, L. Wilk, M. Nusair, *Can. J. Phys.* 58 (1980) 1200-1211.
- [18] P.J. Stephens, F.J. Devlin, C.F. Chabalowski, M.J. Frisch, *J. Phys. Chem.* 98 (1994) 11623-11627.

- [19] S. Huzinaga, J. Chem. Phys. 42 (1965) 1293-1302.
- [20] T.H. Dunning, J. Chem. Phys. 55 (1971) 716-723.
- [21] J. Tomasi, B. Mennucci, R. Cammi, Chem. Rev. 105 (2005) 2999-3093.
- [22] R. Bauernschmitt, R. Ahlrichs, Chem. Phys. Lett. 256 (1996) 454-464.
- [23] J. Autschbach, Chirality 21 (2009) E116-E152.
- [24] P.J. Stephens, N. Harada, Chirality 22 (2010) 229-233.
- [25] J.R. Taylor, Introduction to error analysis, University Science Books, Sausalito, CA, USA, 2<sup>nd</sup> ed., 1997.
- [26] P. Salvadori, C. Bertucci, C. Rosini, in: K. Nakanishi, N. Berova, R.W. Woody (Eds.), Circular dichroism: principles and applications, VCH Publishers, New York, 1994, pp. 541-560.